Stacking solitons in ω-phase systems and quasielastic scattering

B. Horovitz, J. L. Murray,* and J. A. Krumhansl
Laboratory of Atomic and Solid State Physics and Materials Science Center, Cornell University, Ithaca, New York 14853
(Received 27 December 1977)

The unusual x-ray diffuse scattering in Zr-Nb alloys is explained in terms of lattice displacements described by "stacking solitons." These constitute a structural defect in columnar ω-phase regions embedded in a bcc matrix. We model this situation as a one-dimensional system in which a discrepancy between the ω and bcc lattice constants drives the formation of stacking solitons. The density of these solitons depends on composition and temperature; in particular we suggest a commensurate-incommensurate transition at ~17-wt.% Nb, so that the ground state of the higher-percent Nb alloys contains a static array of stacking solitons along the ω-phase column. The dynamics of such configurations is consistent with the very narrow (quasielastic) inelastic scattering observed in these alloys and has the character of a "central peak."

I. INTRODUCTION

Quasielastic scattering appears as a percursor of many structural phase transitions.[1-3] This scattering is of great interest because it arises from the growing short-range order which eventually produces the phase transition; insight into the origin of the quasielastic scattering therefore is insight into the microscopic processes or mechanisms by which the ordering takes place.

Displacive structural transitions are particularly interesting in Zr-Nb alloys.[4-8] These alloys transform from a bcc (β) into a hcp structure below ~610 °C. However, when alloys with 5–30-wt.% Nb are quenched from their high-temperature bcc phase into room temperature, regions of the so-called "ω phase" appear, imbedded in a bcc matrix. The ω phase is a trigonal modification obtained from a bcc structure by adding a displacement modulation with a wave vector $\vec{q}_0 = (1,1,1)(2\pi/3a)$ (Fig. 1).

The ω structure has been studied extensively by neutron,[4] electron,[5,8] x-ray[6] and Mössbauer[7] techniques. The interesting features of the experimental data are the following: (a) As Nb concentration increases the ω-phase reflections become more diffuse and tend to elongate perpendicular to one of the [111] directions. (b) In the 5–15-wt.%-Nb alloys the ω reflections appear at (or very close to) the expected positions of the ω structure, while in the 20–30-wt.% Nb the diffuse peaks are shifted away from these positions. This suggests some kind of transition at about 17-wt.% Nb. (c) As temperature is lowered to ~5 °K the peak position of the 30-wt.% alloy is hardly affected, while the peak shift in the 20-wt.% alloy becomes somewhat smaller.[9] (d) The diffuse peaks are elastic within 3×10^{-9} eV (at room temperature).[7]

The shape of the ω-phase reflections [feature (a)] shows that the ω phase appears in rod-shaped clusters[5,6] along the [111] (β) direction. Thus we assume that the ω clusters are one-dimensional (1D) objects which interact with the surrounding β matrix. We do not use a microscopic theory for the β-ω transition. Instead we assume that the ω phase prefers a smaller lattice parameter than that of the β phase. It will turn out that this information is enough to construct an effective Hamiltonian for an appropriate phase variable in terms of which the scattering can be explained. This effective Hamiltonian leads to the well-known nonlinear soliton solutions[10-12] which we call here stacking solitons. We then show that stacking solitons are stabilized if the discrepancy δ in the lattice constants is larger than some δ_c, and then the ground state is an array of solitons. Thus for $\delta < \delta_c$ the β and ω phase are commensurate, while for $\delta > \delta_c$ they are incommensurate.

The idea of the soliton array or soliton lattice has been used previously to describe dislocations[10] and commensurate-incommensurate transitions of charge-density waves.[12] The appearance of these solitons is a phase transition in the ground state of the system.[12] A study of the thermodynamics of solitons[11] shows that at finite temperature there is no sharp transition, as expected in a 1D system.

In general, the interaction of two incommensurate structures tends to form solitons.[10,12] In our model these two structures are the ω and β phases; thus the model is relevant to the nucleation process, i.e., the disordered phase above some transition temperature.

We begin in Sec. II by reviewing in more detail the experimental data and discussing a (soliton) type of defect proposed by Borie, Sass, and Andreassen[13] (BSA). The BSA defect was given as an *ad hoc* explanation of the x-ray data, with no physical basis. In Sec. III we derive the effective Hamiltonian which

yields different structural defects—the stacking solitons (Fig. 2). In Sec. IV we discuss the correspondence between our theory and the experimental data. We suggest that the critical discrepancy of lattice constants happens at ~17-wt.% Nb, namely, this is the critical concentration for a commensurate-incommensurate transition.[12] In Sec. IV we discuss the nontrivial effect of finite temperatures[11] and suggest a few experiments which can prove (or disprove) the present theory.

II. ω PHASE

In this section, we review the experimental data on the ω phase and the meaning of the proposed BSA defect.[13] Unless otherwise specified, all data correspond to room temperature.

The ω phase can be described by considering the (111) planes of the bcc lattice, which form a sequence of the type $ABCABCA\cdots$ (Fig. 1). The A-A separation is the nearest-neighbor distance in the bcc $3a$, where a is the nearest (111)-plane distance in the bcc. The ω_1 subvariant[13] is formed by collapsing the B-C planes towards their midplane while the A planes remain unshifted. The ω_2 and ω_3 subvariants are formed by retaining the B or C planes, respectively, and collapsing the other pairs of planes.

The ω structure corresponds to a longitudinal displacement modulation in the [111] direction of the form $u\sin(\frac{2}{3}\pi n+\phi)$, where n indexes the (111) planes and $\phi=0$, $\frac{2}{3}\pi$, $\frac{4}{3}\pi$ for the three possible subvariants. In the ideal ω phase $u=u_m\equiv a/\sqrt{3}$ and pairs of planes are fully collapsed to form an hexagonal structure. For a partial collapse $u<u_m$ and the structure is trigonal.

Analysis of the ω reflection intensities[6] shows that u is close to u_m for the 8-wt.% alloy, decreases to $\sim\frac{1}{2}u_m$ for the 20-wt.% alloy, and remains $\sim\frac{1}{2}u_m$ for the 30-wt.% alloy. This may be related to the change of behavior at the ~17-wt.% alloy; at this concentration a sharp anomaly in hardness measurements is also seen.[14]

The ω regions can nucleate in four variants along each of the four equivalent bcc [111] axes; thus, it is natural to use hexagonal notation[6] with the [001] axis is along say [111] (β). For reciprocal-space wave vectors $(0,0,k)$ (in units of $2\pi/a$) the β peaks are at $(0,0,3m)$ while ω scatters at the additional $(0,0,3m\pm1)$ points (m is an integer). The β peaks are much stronger and sharper than the ω peaks, hence the ω phase is formed of clusters imbedded within a bcc matrix. The scattering regions in reciprocal space tend to elongate perpendicular to the [001] axis and this tendency is more pronounced as the Nb concentration is increased; this indicates rod-shaped ω clusters with their long dimension parallel to the [001] axis. Indeed the rod-shaped ω clusters have been seen by direct imaging of electron scattering, even on the 8-wt.% alloy.[8] Thus, we concentrate on the scattering data along $(0,0,k)$ as they contain most of the relevant information.

The shift in position of the ω peak from the expected $(0,0,3m\pm1)$ points is an extremely important feature. In the 5–12-wt.% alloys the ω reflections

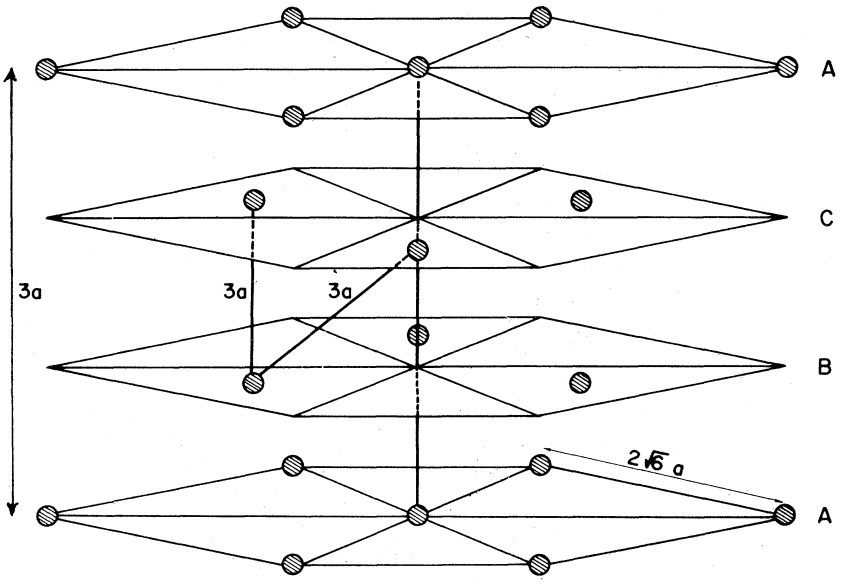

FIG. 1. bcc structure viewed along its [111] direction. For convenience the [111] axis is expanded by a factor of 3 relative to the perpendicular axes. The nearest-neighbor distance is $3a$. The ω phase is obtained by collapsing planes B, C, while planes A are unshifted.

are at the expected positions, i.e., commensurate with the β reference lattice. In the 15-wt.% alloy the peaks shift very slightly, while in the 20 and 30-wt.% alloys the diffuse peaks are shifted considerably. Furthermore, the (0,0,2) and (0,0,5) peaks are shifted to lower wave vectors while the (0,0,1) peak is shifted to a higher wave vector. Unfortunately, the (0,0,4) peak is not visible due to the particular value of u, $u \simeq \frac{1}{2}u_m$. The shifts correspond to an increase of the ω wave vector (or distance from nearest β point) from $q_0 = 2\pi/3a$ to $q_0 + \delta k$, where $\delta k/q_0 \simeq 4\%-6\%$. Thus δk measures the incommensurability from the β lattice.

Now x-ray studies on the 20- and 30-wt.% alloys[9] show that lowering the temperature to $\sim 5\,^\circ$K does not change the general shape of the diffuse scattering and the β-ω transition remains uncompleted. Furthermore, the peak shift of the 30-wt.% alloy does not change, while the peak shift of the 20-wt.% alloy is somewhat reduced but it is definitely present even at $5\,^\circ$K. This indicates that the cause of these peak shifts must be intrinsic to the $T=0$ ground state. An additional clue is provided by the BSA analysis.[13] They found that the correct shifts in the diffuse scattering can be reproduced only if a very particular sequence of subvariants $\omega_1, \omega_3, \omega_2, \omega_1, \cdots$ exists along the ω cluster [Fig. 2(a)]. If the positions of the (111) planes are described by

$$x_n = na + u\sin(q_0 na + \phi_n) \quad , \tag{1}$$

then as n increases the BSA defect sequence implies that ϕ_n jumps by $+\frac{2}{3}\pi$ from one subvariant to the next. Solitons (or kinks) are configurations which interpolate between degenerate ground states.[11,15] Since subvariants are degenerate ground states a jump in ϕ_n which shifts the displacement pattern may be thought of as a soliton.[16] An antisoliton, which would vary locally from 0 to $-\frac{2}{3}\pi$ is not compatible with the BSA sequence. In fact, the form (1) implies immediately that a monotonically increasing function ϕ_n leads to a local wave vector which is larger than q_0, and this leads immediately to the observed shifts in the diffuse peak positions.

The BSA sequence was developed as an *ad hoc* explanation for the shifts in the diffuse peaks. This sequence, viewed as a soliton, is a proper excitation mode, however, it is not acceptable here for the following reasons: (a) individual solitons can be thermally excited but are not a property of the ground state. This contradicts the experiment. (b) There is no reason for the system to prefer solitons to antisolitons; if present in equal numbers the peaks would not be shifted. This also contradicts experiment and the BSA model.

It was suggested by Cook[17] that the bcc instability is associated with a phonon mode whose wave vector q_m differs from q_0. Such a modulation q_m is incommensurate with the lattice and solitons could result.[16] However, the Mössbauer spectroscopy[6,7] shows that the inelastic scattering is centered at the exact ω positions, although the elastic portion is shifted from these positions. Therefore the phonon intensity is centered at q_0 and not at q_m.

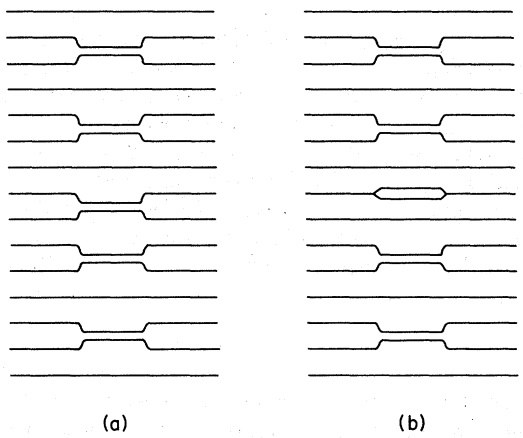

FIG. 2. Defects in an ω-phase cluster embedded in the bcc (111) planes. (a) The BSA structure (Ref. 13) representing a defect in the modulation pattern. (b) The stacking soliton—the ω modulation pattern is maintained but there is a local-density defect. Note that away from the defects the structures (a) and (b) are in exact registry. Hence the structure factors of (a) and (b) are very similar.

In the present theory we concentrate on static properties—we are going to assume that the ω cluster tends to have a smaller lattice constant than the β matrix so that the β-ω interphase interaction stabilizes the stacking soliton array [Fig. 2(b)]. Let us now present some indirect evidence that this assumption is correct.

When the ideal ω phase is formed, the nearest-neighbor distance (within the collapsed planes) becomes smaller by a factor of $\sqrt{8/9} \simeq 0.94$. Therefore it is plausible that the A-A distance in the ω phase will become smaller too.

Structures with smaller lattice separations are favored by applying pressure. This is indeed the case of the ω phase: Under high pressure, pure Zr (hcp phase) transforms into the ω phase.[18] On release of pressure the ω phase persists at room temperature, and is denser than the hcp phase.

The Nb atoms are smaller than the Zr atoms and therefore act as a pressure source. This explains why the ω clusters appear only above 5-wt.% Nb concentration: a finite pressure is needed to induce the ω phase. This also explains the formation of "aged" ω phase[14]: Aging of the alloys at $\sim 500\,^\circ$C leads to big ω clusters with a fixed composition of 6–7-wt.% Nb, while the composition of the β matrix is enriched with Nb. The effect on the 20.7-wt.% alloy is quite spectacular—the β phase is enriched up to 80–90-

wt.% Nb.[19] Thus quenched alloys with more than ~7-wt.% Nb have ω clusters with excess amount of Nb. This leads to excess pressure on the ω cluster and to a tendency of form a smaller lattice constant.

The effect of additional impurities was studied by Buck *et al.*[18] They find that oxygen suppresses the ω formation temperature, while hydrogen raises it. This is consistent with our theory—H atoms prefer shorter bonds and help to nucleate the ω clusters, while O atoms prefer longer bonds, which are not favored by the ω phase.

III. STACKING SOLITONS

In this section we study a model 1D chain with a natural lattice parameter $a-\delta$ nucleated in a matrix with a lattice parameter a. In addition the chain is formed from the matrix by a periodic displacement modulation with a wave vector $q_0=2\pi r/a$, where r is a rational number. This is similar to a 1D epitaxy problem[20] except that here the very existence of the chain is due to an instability of the matrix. Thus the change in the lattice parameter is intrinsic to the phase transition, and must be described by the displacement field itself—the "order parameter" of this problem.

The average positions of the atoms in the chain are specified by a sequence $\langle x_n\rangle$ from which the displacement modulation is defined. The values $\langle x_n\rangle$ are not necessarily separated by $a-\delta$, since the matrix strains the chain and prefers values of $\langle x_n\rangle$ separated by a. The actual positions of the atoms are $x_n=\langle x_n\rangle+u_n\sin(q_0\langle x_n\rangle+\phi_n)$, and in general u_n and ϕ_n are position-dependent amplitude and phase of the order parameter. Variations in the amplitude require usually more energy than phase variations,[21] and therefore we now consider the simpler case $u_n=\text{const}=\bar{u}$. In Sec. V we discuss the effects of amplitude modulation.

The important physics is that variations in ϕ_n are coupled to variations in the density. This is derived from the identification of the local wave-vector with the local lattice constant by the relationship

$$q_0 a = q_{\text{loc}} a_{\text{loc}} \ , \tag{2}$$

where

$$a_{\text{loc}} = \langle x_{n+1}\rangle - \langle x_n\rangle$$

and

$$q_{\text{loc}} = q_0 + (\phi_{n+1}-\phi_n)/a_{\text{loc}} \ . \tag{3}$$

Note that the modulation pattern is defined by r (for the ω phase $r=\frac{1}{3}$), and is independent of $\langle x_n\rangle$. Equation (2) means that this pattern on the chain is indeed locked into its own lattice, in spite of possible shifts in the positions $\langle x_n\rangle$. Equations (2) and (3) lead to

$$\langle x_n\rangle = na - \phi_n/q_0 \ , \tag{4}$$

$$a_{\text{loc}} = a - (\phi_{n+1}-\phi_n)/q_0 \ . \tag{5}$$

The relation (5) between variations in the phase and the local density in a continuum limit is well known for charge density wave systems.[21,22] From Eq. (4) we obtain the following equivalent relations:

$$x_n = na + \bar{u}\sin(q_0\langle x_n\rangle + \phi_n) - \phi_n/q_0 \ , \tag{6}$$

$$x_n = na + \bar{u}\sin(2\pi r n) - \phi_n/q_0 \ . \tag{7}$$

These results are different from the form (1). In particular, a solution for ϕ_n which varies from 0 to $q_0 a$ leads to the BSA defect in Eq. (1) while in Eq. (7) there is no defect in the modulation pattern; it is the density which is modified locally (Fig. 2). This demonstrates the physics behind Eq. (2): The phase is locked to its own lattice, i.e., the chain, but may be unlocked relative to the surrounding matrix. Therefore, the BSA-type solitons are not allowed in this scheme, but instead we can obtain "stacking solitons," that is, solitons in the phase of the chain relative to the surrounding matrix.

If the transformed chain were free to have its own lattice constant $a-\delta$, then Eq. (4) yields $\phi_n=q_0 n\delta$ and $x_n=n(a-\delta)+u\sin(2\pi r n)$. However, the surrounding matrix tries to lock the chain into the lattice periodicity a so that $\phi_n=aq_0K=\text{const}$, where K is an integer. We proceed now to show that the compromise between these competing forces is a soliton array, as illustrated in Fig. 3(a).

The locking energy V_{lock} is a periodic function of the shift $\langle x_n\rangle - na$ with periodicity a. (The additional shift u is omitted here since it contributes to the u dependent energies.) A simple form is

$$-\cos[2\pi(\langle x_n\rangle - na)/a] \ ,$$

so that

$$V_{\text{lock}} = \omega_0^2[1-\cos(\phi_n/r)] \ . \tag{8}$$

This form can also be obtained from a Landau free energy expansion[12] with umklapp coupling to the surrounding matrix; e.g., for $r=\frac{1}{3}$ the order parameter $u\exp(i\langle x_n\rangle 2\pi/3a + i\phi_n)$ to the third power is coupled to the matrix potential with wave vector $2\pi/a$ and leads to an energy term $\sim\cos(3\phi_n)$.

The competing phase dependent energy is the elastic energy of the form $\frac{1}{2}C[\langle x_{n+1}\rangle - \langle x_n\rangle - (a-\delta)]^2/a^2$. Thus we are led to the following phase-dependent Hamiltonian

$$H = \sum_n \left[\frac{C}{8\pi^2}(\psi_{n+1}-\psi_n)^2 + \omega_0^2(1-\cos\psi_n)\right] - \frac{C}{2\pi}\frac{\delta}{a}(\psi_N - \psi_{-N}) \ , \tag{9}$$

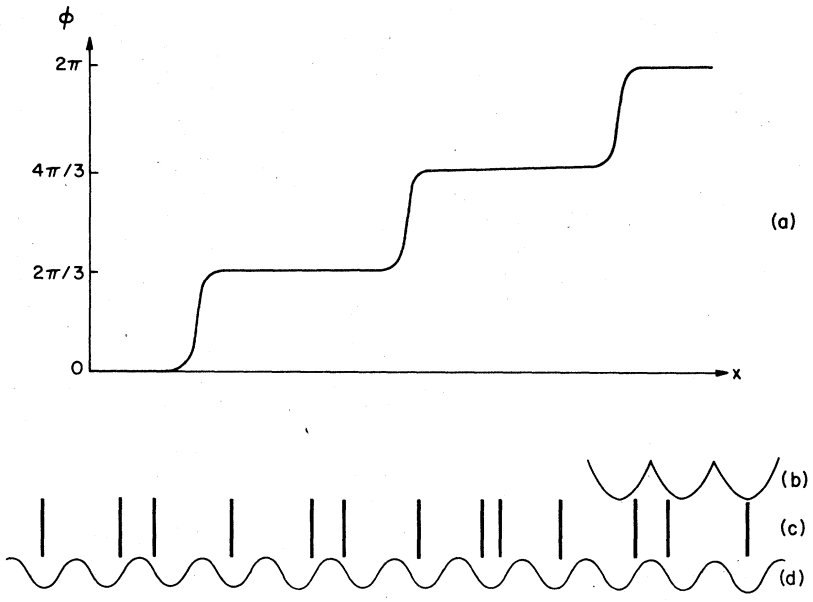

FIG. 3. Soliton solutions for Eq. (10) where $\Psi_n = 3\phi_n$. (a) The soliton array in the continuum model. (b) The approximate potential of Eq. (11). (c) The actual positions which correspond to a stacking soliton, as described by Eqs. (7), (13), or (17). The modulation pattern $[u \sin(\frac{2}{3}\pi n)]$ is maintained but there is a local density increase [as in Fig. 2(b)]. (d) The locking potential of the surrounding matrix as felt by the atoms in the chain (c).

where $\psi_n = \phi_n / r$. The effects of time dependence are discussed later.

In the last term of Eq. (9), $\psi_N - \psi_{-N}$ is the phase difference of the first and last atom in the chain and measures the length change [Eq. (4)]. Therefore δ is identified as the pressure on the chain, and positive pressure ($\delta > 0$) favors increasing solutions ψ_n and length contraction.

The Hamiltonian [Eq. (9)] can be derived directly from Eq. (11) without identifying ϕ_n as a phase. This actually has been done[10] and the resulting structures have been identified as dislocations. Our approach shows that changes in the lattice constant are coupled intrinsically to the phase of a complex order parameter and therefore the solutions of Eq. (9) appear in the nucleation process of a phase transition.

The equation of equilibrium for the phase field ψ is

$$\psi_{n+1} + \psi_{n-1} - 2\psi_n = (4\pi^2 \omega_0^2 / C) \sin\psi_n \ . \qquad (10)$$

The continuum limit of this equation is the sine-Gordon equation which has been extensively studied.[10–12,15] The single soliton or antisoliton solutions are $\psi(x) = 4 \tan^{-1}[\exp(\pm x/l)]$, $l = a\sqrt{C}/2\pi\omega_0$, and their variations from 0 to $\pm 2\pi$ are localized around $x = 0$ with a width of $\sim 2l$. The energy of a soliton (for $\delta = 0$) is $4\omega_0\sqrt{C}/\pi$, but the pressure term reduces this energy by $C\delta/a$. Therefore, if δ is large enough, $\delta > \delta_c$ where $\delta_c/a = 2a/\pi^2 l$, solitons appear in the ground state. Since solitons repel each other the ground state is an infinite lattice of solitons.[10–12] (Clearly, if $\delta < -\delta_c$ an array of antisolitons will appear.) Thus we obtain a transition in the ground-state properties of the chain. For $|\delta| < \delta_c$ there are no solitons and the phase is locked $\psi(X) = \text{const}$, while for $\delta > \delta_c$ a soliton lattice appears. As δ grows the soliton density increases, until for $\delta/\delta_c \to \infty$ the solitons merge into a line $\psi(X) = 2\pi\delta x/a^2$ which is the free chain with its lattice constant $a - \delta$.

The lock-in transition concept has been used to describe transitions of charge-density waves from incommensurate to commensurate waves relative to the lattice.[12] The wave vector of the density wave, as determined by the soliton density, approaches the lattice wave vector as $|\delta|$ approaches δ_c from above; at $\delta = \delta_c$ the solitons disappear and the density wave is locked in.

In the case of charge-density waves a continuum description is appropriate for the electron gas, while here we have a discrete lattice for which the solution is, in general, much more difficult. However, an explicit solution is available[20] if the locking potential is taken to be a periodic array of parabolas [Fig. 3(b)]

$$V_{\text{lock}} = 2\pi^2 \omega_0^2 [\psi_n / 2\pi - \mu(\psi_n)]^2 \ , \qquad (11)$$

where $\mu(\psi_n) = \text{Int}(\psi_n/2\pi + \frac{1}{2})$ and $\text{Int}(x)$ is the integer nearest to x. The equation of motion is now

$$\psi_{n+1} + \psi_{n-1} - 2\psi_n = (4\pi^2 \omega_0^2 / C)[\psi_n - 2\pi\mu(\psi_n)] \ . \qquad (12)$$

The single-soliton solution has the form

$$\frac{\psi_n}{2\pi}=\begin{cases}1-\lambda^{n-n_0}/(1+\lambda)\ , & n>n_0\\ \lambda^{n_0-n+1}/(1+\lambda)\ , & n\leq n_0\end{cases}\ , \tag{13}$$

where $\lambda<1$ solves $\lambda/(1-\lambda)^2=C/(2\pi\omega_0)^2$. This solution describes an increase of ψ_n by 2π localized near n_0. In terms of the positions $\langle x_n\rangle$ the soliton describes a contraction of the chain by one lattice spacing a, the density increase is localized near n_0 [Fig. 3(c)]. The soliton energy (for $\delta=0$) is

$$E_s=\tfrac{1}{2}C(1-\lambda)/(1+\lambda)\ . \tag{14}$$

In the continuum limit, $C\gg\omega_0^2$ or $\lambda\to1$, the soliton is wide and the discontinuity in the derivative of the potential Eq. (11) is felt more strongly. However, even in this limit E_s differs from the exact result of the $\cos\psi_n$ potential just by a factor of $8/\pi^2$; hence the potential Eq. (11) is a good approximation for the potential Eq. (8), at least for static solutions.

The pressure term in Eq. (9) reduces the soliton energy by $C\delta/a$ so that the soliton lattice is the ground state of the chain for

$$\delta/a>\tfrac{1}{2}(1-\lambda)/(1+\lambda)\equiv\delta_c/a\ . \tag{15}$$

Until now we discussed only static solutions. If we add a term $\sim(\partial\psi_n/\partial t)^2$ to Eq. (9), in the continuum limit the solitons can move with velocities up to the sound velocity. This implies that the translation mode has zero frequency and the oscillations of the soliton lattice form a band with frequencies ≥0.[11] This band is narrow if the density of solitons is low, namely, $\delta(>\delta_c)$ is close to δ_c.

The solitons of the discrete problem (with a well-behaved potential) are free to move only if C/ω_0^2 is not too small,[20] and solitons which are too narrow relative to the lattice spacing are locked and their translation requires a finite energy. Hence the excitation spectrum begins at some finite frequency.

In Sec. IV, we show that the solitons in the ω phase are very narrow and therefore they form a static configuration. This is consistent with the experimental feature (d): the extreme narrowness of the quasielastic peak.

IV. STACKING SOLITONS IN THE ω PHASE

As discussed in Sec. II, we consider the small Nb atoms as the source of the pressure term in Eq. (9). We assume that the randomly distributed Nb atoms lead to a homogeneous pressure which implies that the ω cluster tends to have a smaller lattice constant. As shown in Sec. III, above some critical pressure stacking solitons exist in the ground state of the system. The critical pressure corresponds to about 17-wt.% Nb and explains the transition as Nb concentration is changed [feature (b)].

We proceed now to evaluate the diffuse scattering from the high-percent Nb alloys. In order to apply the theory of Sec. III we make some additional approximations: (a) the ω cluster is long enough compared with the lattice constant and the soliton width. Therefore, the effects of the end atoms on the amplitude u and the soliton solution can be neglected. The parameters which we obtain below [in Figs. 4 and 5] justify this approximation. (b) Each plane within the ω cluster consists of a small and equal number of atoms so that the locking potential is constant within this plane and has the periodicity a [Fig. 3(d)]. This is consistent with the observed rod-shaped ω cluster.[6,8] The main elastic energy for atomic shifts along the cluster is between "third-nearest" planes since these planes contain nearest-neighbor atoms along the chain; (e.g., see the A planes in Fig. 1). The Hamiltonian Eq. (9) is then modified to

$$H=\sum_n\left[\frac{C}{8\pi^2}(\phi_{n+3}-\phi_n)^2+V_{\text{lock}}(3\phi_n)\right]-\frac{3C}{2\pi}\frac{\delta}{a}(\phi_N-\phi_{-N})\ . \tag{16}$$

For the potential Eq. (11) the single-soliton solution is

$$\frac{3\phi_n}{2\pi}=\begin{cases}1-\lambda_1^{n-n_0}/(1+\lambda_1^3)\ , & n>n_0+1\\ \lambda_1^{3+n_0-n}/(1+\lambda_1^3)\ , & n\leq n_0+1\end{cases}\ , \tag{17}$$

where $\lambda_1<1$ solves $\lambda_1^3/(1-\lambda_1^3)^2=C/(6\pi\omega_0)^2$. This solution is shown in Fig. 3(c). The energy of Eq. (17) is $\frac{1}{6}C(1-\lambda_1^3)/(1+\lambda_1^3)$ and therefore the condition for solitons in the ground state is

$$\delta/a>\tfrac{1}{6}(1-\lambda_1^3)/(1+\lambda_1^3)\equiv\delta_c/a\ . \tag{18}$$

The scattering intensity is given by

$$S(k)=\left|\sum_n e^{ikx_n}-\sum_n e^{ikna}\right|^2\ , \tag{19}$$

where the summation is on the planes in the ω cluster and x_n is given by Eqs. (7) and (17). The last term of Eq. (19) is the missing bcc scattering, and the remainder—the ideal bcc scattering—is not relevant to the diffuse scattering. The solitons are assumed to be far apart compared to their width ($\delta\simeq\delta_c$) so that the many-soliton solution consists of the single-soliton solutions [Eq. (17)] at the appropriate positions. Equation (19) is plotted in Figs. 4 and 5 for $\lambda_1=0.2$, $u=\frac{1}{2}u_m$, and $M=0,1,2$ solitons in an ω cluster with 40 planes.

Since the phase appears in Eq. (6) in two places there are two types of peak shifts. For a soliton (increasing function ϕ_n) the local wave vector [Eq. (3)]

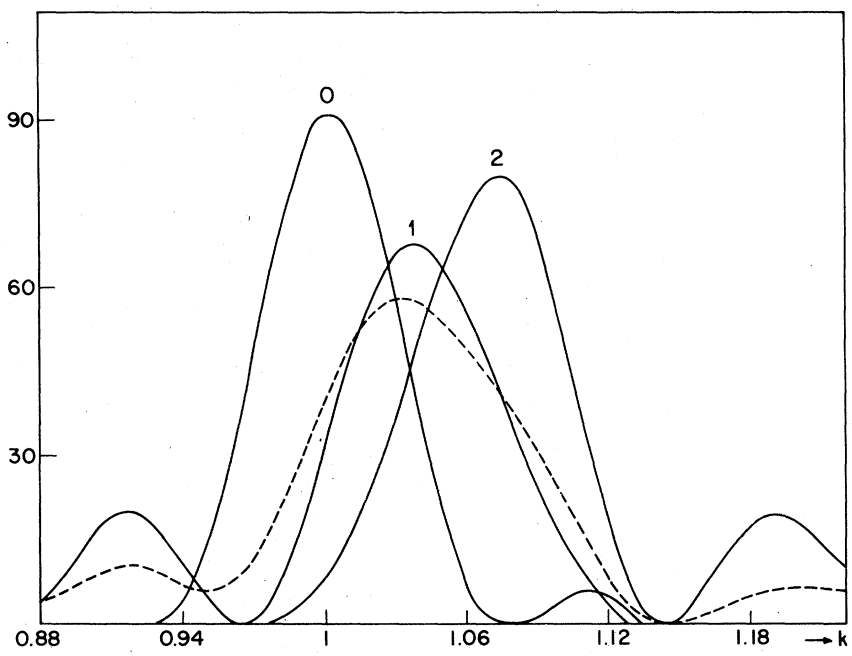

FIG. 4. Scattering intensity of the (001) peak [Eq. (19)]. k is in units of $q_0=2\pi/3a$, $\lambda_1=0.2$, $u=\frac{1}{2}u_m$. The full curves correspond to $M=0,1,2$ solitons in a 40-plane ω cluster. For $M=1$ the soliton is at the center of the cluster and for $M=2$ the soliton are at $\sim\frac{1}{4}$ and $\sim\frac{3}{4}$ of the cluster. The dashed line is an average with 25% $M=0$, 50% $M=1$, and 25% $M=2$. The side peaks are due to second harmonics and are noticeable due to the weak intensity of this reflection.

is larger than q_0 and the ω peak shifts away from the nearest bcc reflection ("phase-shifted" peak). The second effect leads to a locally smaller lattice constant [Eq. (5)] and a shift of the ω peaks away from the origin in reciprocal space ("density-shifted" peaks). For the (0,0,1) peak both shifts are in the same direction and we expect a single peak as in Fig. 4. Note that this peak is much weaker than the (002) peak and side peaks due to second harmonics are noticeable on this scale. For the (0,0,2) peak the two effects lead to shifts in opposite directions as in Fig. 5. The soliton with $\lambda_1=0.2$ is very narrow so that the density change is limited to a small region; hence the phase-shifted peak dominates in Fig. 5. As λ_1 increases the solitons become wider; the intensity of the density-shifted peak grows while the phase-shifted peak is diminished. In the limit $\lambda_1\to 1$ ($\omega_0^2/C\to 0$) the solution $\phi_n=2\pi n\delta/3a$ describes a free ω cluster with density-shifted peaks at $2\pi n/3(a-\delta)$ and no phase-shifted peaks.

Experimentally the (0,0,2) peak is shifted down which implies that the phase-shifted peak dominates and the soliton is narrow. Also the experimental peak is slightly asymmetric but there are no additional peaks.[6,9] Therefore, we assume that the various ω clusters (for a given % Nb alloy) contain different number of solitons. As shown by the dashed curve in Fig. 5 the phase-shifted peaks add up while the density-shifted peaks are smeared and the net result is an asymmetric peak. Further reduction in the value of λ_1 reduces the amount of asymmetry.

Our results for the diffuse peaks at the bcc reflection points $(0,0,3n)$ with $\lambda_1=0.2$ give a symmetric peak centered around the exact bcc point. For these reflections there is no phase shifting while the density-shifted peak is very small for $\lambda_1=0.2$. For a larger value of λ_1 the solitons are wider and a density shifted peak appears *above* the bcc reflection points.

The shift in the (002) peak can also be explained by antisolitons which appear in the ground state for $\delta<-\delta_c$. Then a wide antisoliton, which tends to have a lattice parameter $a+|\delta|$, yields a dominant density-shifted peak in the right direction. This seems to be a feature of another proposed defect of the ω cluster.[8,23] However, in this case the (001) peak would also shift down and an additional peak below the bcc reflections would appear. Both of these features do not agree with the experimental data.

In conclusion the main features of the x-ray diffuse scattering are explained by a *narrow soliton* structure. In fact, this structure is almost the same as the BSA defect except for one additional plane (see Fig. 2). This difference has a small effect on the scattering intensity and therefore both structures yield similarly good fits to the experimental data.

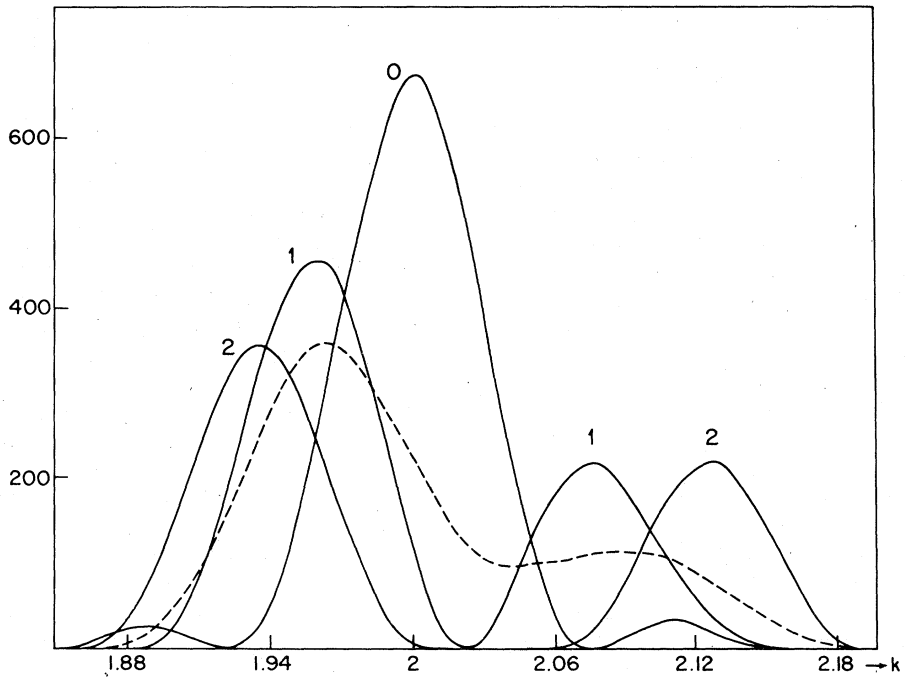

FIG. 5. Same as Fig. 4 for the (002) peak. The peaks to the left are "phase shifted," while those to the right are "density shifted." For a smaller λ_1 the density-shifted peaks become even smaller compared to the phase-shifted peaks. The average dashed curve shows that the average cluster behavior in a given alloy can lead to a single asymmetric peak.

V. DISCUSSION

The theory presented in this work is able to account for the experimental features of the ω phase, as presented in Sec. I, in terms of stacking solitons. The low-% Nb alloys have rather long rod shaped ω clusters[5,6,8] so that parallel clusters can be correlated by clusters of other $\langle 111\rangle$ (β) variants and the scattering appears to be three-dimensional (3D). As the Nb concentration increases the clusters become shorter,[5,6,8] although their diameter hardly changes.[5] Hence the clusters become less correlated and the scattering appears to be more 1D—elongated perpendicular to the [111] (β) axis. The rod-shaped ω clusters, which exist in all the quenched alloys, are the basis for our 1D theory.

The theory assumes that the ω clusters tend to have a smaller lattice constant than that of the β matrix. If the difference δ in the lattice constants is too small the ω cluster is completely locked into the β matrix and there are no solitons. This corresponds to the low-percent Nb alloys. If δ is large enough solitons appear in the ground state, partially unlocking the ω cluster from the β matrix. This corresponds to the high-percent Nb alloys and explains their shifted ω peaks. Thus we view the transition of $\sim$17-wt.% Nb as a commensurate-incommensurate transition.[12]

The critical value δ_c/a from Eq. (18) with $\lambda_1=0.2$ is $\sim$16%. This is an overestimate since we did not consider variations in the displacement amplitude u and the soliton transverse shifts (three-dimensional (3D) effects). These are additional degrees of freedom which by readjusting lead to a lower soliton energy and therefore a lower critical δ_c. For example, the locking energy $\sim -u^3\cos 3\phi$ is minimized at $u>0$ and $3\phi = 2\pi K$, where K is an integer. As $\phi=\phi_n$ deviates from this minimum in the soliton region, the increase in the locking energy is reduced by a smaller u. Thus the soliton involves a phase change and a local reduction in the amplitude. This is a general feature of the coupled phase-amplitude problem.[21]

The phase-amplitude coupling affects the modulated planes (planes B,C in Fig. 1) so that most of the soliton energy involves the unmodulated planes (planes A in Fig. 1). Therefore, the soliton energy may be reduced by a factor of $\sim\frac{1}{3}$ and we estimate the critical difference in lattice constants to be $\delta_c/a \simeq 5\%$.

A quantitative theory should be a 3D theory of a coupled amplitude-phase problem. However, the results for the diffuse scattering are insensitive to the details of the soliton shape. Using Eq. (13) or the continuum solution instead of Eq. (17) yields similar scattering intensities. Therefore, the theory is quali-

tatively correct, and enables us to account for the shift in the diffuse scattering.

The stacking solitons are presented in Sec. III as a ground-state property of the system. In order to study the finite temperature behavior we assume that the amplitude $\bar{u}$ depends weakly on temperature, which is consistent with experiment.[9] Therefore, the coefficients in the effective Hamiltonian Eq. (9) are assumed to be constants, and the main temperature dependence comes from the $1/T$ factor in the partition function. (This is quite different from the temperature dependence in Ref. 12; there the $T=0$ solution is used with the parameter δ/E_s changing with temperature.)

In general, we expect the soliton density to be a sensitive function of temperature for $\delta \sim \delta_c$. In this case the interaction between solitons is weak and the net energy for creation or annihilation of a soliton is close to zero. This temperature dependence has been evaluated for the continuum model.[11] At $T=0\,^\circ$K the soliton density $\rho(\delta)$ jumps from $\rho=0$ at $\delta=\delta_c$ with infinite slope, while for $T\neq 0\,^\circ$K, ρ increases from $\delta=0$ and is analytic for all δ. This reflects the fact that there are no sharp transitions in 1D systems for $T\neq 0\,^\circ$K.

The temperature effect can explain why the transition as Nb concentration changes is not sharp, and we expect it to sharpen up at low temperatures. Thus we expect that the slight peak shift of the 15-wt.% alloy will disappear at low temperatures. The alloy with $\sim$17-wt.% should be the most sensitive to temperature changes. The 20-wt.% alloy has δ close to δ_c and therefore its peak shift changes with temperature. The 30-wt.% alloy has δ far from δ_c and its peak shift should depend weakly on temperature. These results for the 20 and 30-wt.% alloys were indeed seen in a recent experiment.[9]

The proposed solitons are very narrow and then the discreteness of the problem leads to a static configuration.[20] This explains the last of the experimental features, as presented in Sec. I.

In order to prove our assumption about the lattice constant of the ω cluster one should find a direct β-ω transition. This transition occurs upon aging, as discussed in Sec. II, but this process involves Nb diffusion from the ω phase into the β phase. The excess Nb atoms in the ω clusters of the quenched alloys is the source of the pressure and the tendency to form a smaller lattice constant. Therefore, one should look for a β-ω transition without changes in the ω phase composition.

We therefore suggest the following experiment: Apply high pressure on the quenched Zr-Nb alloys at room temperature and then release the pressure. As in the pure Zr case,[18] the alloy should transform into a 3D ω phase, and this phase should be retained after the pressure release. In this experiment the Nb distribution does not change. Therefore, we predict that the resulting ω phase will have a smaller lattice constant in its [001] direction than the previous bcc lattice in its [111] direction. The change δ in the lattice constant should increase with Nb concentration and the critical δ_c at $\sim$17-wt.% Nb can be determined. This experiment, if successful, will confirm our theory and solve the puzzle of the ω phase.

Finally we suggest that stacking solitons are relevant to the general problem of the central peak. Evidently we look for transitions which involve a change in the lattice constant, but this is probably true for all displacive transitions. Also one should study the appearance of stacking solitons on a surface of 3D clusters.[24]

The central peak is the peak in the scattering $S(q_0,\omega)$ around frequency $\omega=0$, at temperatures above a displacive phase transition; it is usually associated with the dynamics of domains which are separated by solitons or kinks.[25–27] These kinks connect degenerate states *within* a nucleating phase [e.g., the BSA defect—Fig. 2(a)]. The stacking solitons are very different from these kinks—they result from the interaction *between* one nucleating domain and the untransformed matrix. Furthermore, stacking solitons are favored by the interphase interaction and for $|\delta| > \delta_c$ they are formed spontaneously.

The models for the central peak[25,26] consider 1D systems, and it is still not understood why domains in 3D systems are so stable and quasistatic. These domains can either move around (phase fluctuations) or disappear (amplitude fluctuations). Both phenomena can be seen by computer simulations,[27] and they tend to broaden $S(q_0,\omega)$. Consider now the effect of stacking solitons: If the soliton is not too wide compared with the lattice spacing, translation requires finite energy[20] and phase fluctuations are suppressed; this can happen in a discrete model also without stacking solitons. In addition however, the stacking soliton suppresses also amplitude fluctuations, since by taking the amplitude to zero the density defect is not removed [Fig. 2(b)]. Thus there is an energy barrier against motion or decay of domains, and then the central peak becomes narrower. Experimentally stacking solitons are seen by a shift of the peak in $S(q_0,\omega)$ away from q_0, and we suggest that this shift correlates with increasing narrowness of the peak around $\omega=0$.

A well known example are the A-15 compounds Nb_3Sn and V_3Si,[2,3] which transform from cubic to tetragonal at 45 and 21 °K, respectively. Evidently, this transition involves changes in the lattice constant and stacking solitons are favored. In fact, the central peak was found to exist also away from $q=0$ which is analogous to the shift in the ω reflection peaks. Various properties of this transition were explained by postulating the existence of defects.[28] Stacking solitons are natural and intrinsic structures which can represents these defects.

ACKNOWLEDGMENTS

We thank the following for very useful discussions: S. Aubry, B. W. Batterman, D. H. Bilderback, T. S. Kuan, and S. L. Sass. In particular we are very grateful to D. H. Bilderback and B. W. Batterman for presenting us their unpublished data. This work was supported in part through the Materials Science Center, Cornell University.

---

*Present address: National Bureau of Standards, Washington, D.C. 20234.

[1]For recent reviews see: *Proceedings of the International Conference on Lattice Dynamics, 1977* edited by M. Balkansky, (Flammarion, Paris, to be published).

[2]S. M. Shapiro, J. D. Axe, G. Shirane, and T. Riste, Phys. Rev. B 6, 4332 (1972).

[3]J. D. Axe and G. Shirane, Phys. Rev. B 8, 1965 (1973).

[4]D. T. Keating and S. J. LaPlaca, J. Phys. Chem. Solids 35, 879 (1973).

[5]S. L. Sass, J. Less Common Met. 28, 157 (1972); C. W. Dawson and S. L. Sass, Metall. Trans. 1, 2225 (1970).

[6]W. Lin, H. Spalt and B. W. Batterman, Phys. Rev. B 13, 5158 (1976).

[7]S. K. Andersen and B. W. Batterman, Solid State Commun. 26, 195 (1978).

[8]T. S. Kuan and S. L. Sass, Philos. Mag. 36, 1473 (1977).

[9]D. H. Bilderback and B. W. Batterman (private communication).

[10]F. C. Frank and J. H. van der Merwe, Proc. Roy. Soc. Lond. A 198, 205 (1949).

[11]N. Gupta and B. Sutherland, Phys. Rev. A 14, 1790 (1976).

[12]W. L. McMillan, Phys. Rev. B 14, 1496 (1976); P. Bak and V. J. Emery, Phys. Rev. Lett. 36, 978 (1976); B. Horovitz (unpublished).

[13]B. Borie, S. L. Sass, and A. Andreassen, Acta Crystallogr. A 29, 594 (1973).

[14]D. J. Cometto, G. L. Houze, Jr., and R. F. Hehemann, Trans. Metall. Soc. AIME 30, 233 (1965).

[15]A. C. Scott, F. Y. F. Chu and D. McLaughlin, Proc. IEEE 61, 1443 (1973).

[16]This has also been noticed by R. Pynn, J. Phys. F 8, 1 (1978).

[17]H. E. Cook, Acta Metall. 23, 1041 (1975); J. M. Sanchez and D. DeFontaine, J. Appl. Crystallogr. 10, 220 (1977).

[18]J. C. Jamieson, Science 140, 72 (1963); O. Buck, D. O. Thompson, N. E. Paton, and J. C. Williams, *Proceedings of the 5th International Conference on Internal Friction and Ultrasonic Attenuation in Crystalline Solids* 1975), Vol. 1, p. 451.

[19]B. A. Hatt and V. G. Rivlin, Fulmer Research Inst. Report No. R./219/7 (1967) (unpublished).

[20]S. Aubry, J. Math. Phys. (to be published).

[21]B. Horovitz and J. A. Krumhansl, Solid State Commun. 26, 81 (1978).

[22]T. M. Rice, Solid State Commun. 17, 1055 (1975).

[23]T. S. Kuan and S. L. Sass, Acta Metall. 24, 1053 (1976).

[24]B. Horovitz, J. A. Krumhansl and E. Domany, Phys. Rev. Lett. 38, 778 (1977).

[25]J. A. Krumhansl and J. R. Schrieffer, Phys. Rev. B 11, 3535 (1975).

[26]S. Aubry, J. Chem. Phys. 62, 3217 (1975); 64, 3392 (1976).

[27]T. Schneider and E. Stoll, Phys. Rev. B 13, 1216 (1976).

[28]C. M. Varma, J. C. Phillips and S. T. Chui, Phys. Rev. Lett. 33, 1223 (1974); J. C. Phillips, Solid State Commun. 18, 831 (1976); K. L. Ngai and T. L. Reinecke, Phys. Rev. B 16, 1077 (1977).